A Liquid-Junction-Free Reference Electrode Based on a PEDOT Solid-Contact and Ionogel Capping Membrane

Claudio Zuliani*, Giusy Matzeu, Dermot Diamond*

Clarity Centre for Sensor Web Technologies, National Centre for Sensor Research, Dublin City University, Dublin 9, Ireland

Tel: +353 1 700 6404; Fax: +353 1 700 7995

*Email: c.zuliani@imperial.ac.uk; dermot.diamond@dcu.ie

Abstract.

Liquid-junction-free reference electrodes were prepared on screen printed substrates using poly-3,4-ethylenedioxythiophene (PEDOT) as solid-contact and novel ionogels as capping membrane. The chemico-physical properties of the PEDOT layer were tuned by changing the electropolymerization media and electrodeposition technique. Particularly, electrodepositing PEDOT films potentiostatically or potentiodynamically impacted on the traces of the potential of the electrodes during the conditioning step. In addition, the choice of the capping membrane formulation, e.g., acrylate monomers, ionic liquid, cross-linkers and photo-initiators, was adjusted to obtain electrodes with properties almost equivalent of a standard reference electrode. Thus, calibration plots of Na^+ ion-selective electrodes against the optimized solid-contact ionogel reference electrodes (SCI-REs) or against a double-liquid junction Ag/AgCl electrode did not present any significant difference. Such SCI-REs may provide an effective route to the generation of future low-cost components for potentiometric sensing strips.

Keywords: reference electrode, solid-contact, ionic liquid, ionogel, screen printing, poly-3,4-ethylenedioxythiophene (PEDOT), Ion-Selective Electrode (ISEs)

1. Introduction

In order to realize low-cost potentiometric sensors, a reference electrode compatible with mass production such as screen-printing is required [1]. While there has been considerable success in producing devices based on a disposable single/limited use model, a significant challenge remains in the production of devices capable of continuous use over longer periods of time [1-3]. Improving the performance of commercially available reference electrodes compatible with thin- and thick-film technologies is an issue which has received relatively little attention [4]. There is a need for all solid-state reference electrodes of analytical quality which would retain the performance of a classical reference electrode while offering additional advantages such as maintenance-free use and compatibility with low-cost mass production manufacturing techniques [5].

While minor variations of the salt bridge or junction design [4, 6] may produce some performance improvements, they do not render the design compatible with mass-production and the effectiveness may be relatively short-term. For example, gel-like materials employed in salt bridge electrolytes do commonly suffer from drying and leaching [1, 3]. Mi et al. [7] introduced a novel concept for the preparation of a pseudo-reference using hydrophobic anion-exchanger membranes loaded with the polyanion heparin. Because heparin passively diffuses at a low rate from the ion-exchanger membranes into the sample, the potential drop across the solution/membrane interface is almost sample-independent and well defined [4, 7]. Following this advance, water-immiscible ionic liquids, or hydrophobic polymeric membranes doped with ionic liquids were employed to overcome some of the typical reference electrode limitations described above [4, 8]. For instance, Kakiuchi et al. [9] introduced ionogels based on the bis(trifluoromethanesulfonyl)imide [NTf_2] ionic liquid family as a novel salt-bridge material for reference electrodes. Following this investigation, ionogels based on [NTf_2] ILs [4, 10] were employed as capping membranes in order to prepare disposable solid-contact ionogels reference electrodes (SCI-REs). Since the hydrophobic polymeric membrane contains an ionic liquid which is sparingly soluble in water [10, 11], its partition between the two phases creates a local equilibrium distribution thus establishing a potential, $E_{PB,}$ defined by the phase boundary model [10, 11], see Equation 1:

$$E_{PB} = \frac{RT}{z_I F} ln \frac{k_I \, a_I}{\gamma_I [I^{z_I}]} \quad (1)$$

where k_I is the phase transfer energy, a_I is the activity of an ion of charge z_I in the sample phase, γ_I and $[I^{z_I}]$ are respectively the activity coefficient and the concentration of the free

ion I^{zI} in the membrane phase; *R*, *T*, and *F* are the gas constant, the absolute temperature, and the Faraday constant, respectively.

The use of ionogels to prepare reference electrodes can be seen as an improvement of the lipophilic salt approach introduced by Mattinen et al. [11, 12] since no solvent is required. However, Cicmil et al. [10] showed that electrodes prepared by dropcasting [NTf_2]/PVC ionogels onto a poly(3-octylthiophene-2,5-diyl) (POT) solid contact layer exhibited changes in potential of up to 20-25 mV and 15-20 mV when the concentration of bathing solutions of KCl and NaCl was increased from 1 to 10 mM, respectively. In addition, Zhang et al. [4] showed that protonation of [NTf_2] within the ionogel phase at pH < 4.5 caused transmembrane fluxes which generated significant changes in the electrode potential. In addition, the role of the solid-contact in SCI-REs has not been explored to any great extent.

In this paper, we present evidence to support the view that the type of IL anion employed during the electropolymerization of the conducting polymer (CP) layer (i.e., formation of the SC-layer) affects the performance of the resulting electrodes, when tested in comparison to a commercial double-junction reference electrode. We also demonstrate that the variation in the potential of the electrodes in contact with Na^+ and K^+ chloride salts solutions can be reduced through careful formulation of the membrane components, e.g., through choice of the IL used in the ionogel capping layer, and the nature of the underlying solid-contact material. Such optimized electrodes are finally shown to perform well as reference electrodes for the potentiometric calibration of NaCl solutions using Na^+-ion-selective electrodes (Na^+-ISEs) and for the measurement of pH in real-saliva samples.

2. Experimental

2.1 Materials

The C2030519P4 carbon ink and the D50706D2 dielectric ink from Gwent Electronic Materials (Pontypool, UK) were used to prepare screen printed electrodes. 175 μm thick PET sheets from HiFi (Dublin, Ireland) or MacDermid (Oxon, UK) were employed as substrates for screen-printing. Potassium and sodium chloride, 3,4-ethylenedioxythiophene (EDOT, 97%), poly(3-octylthiophene-2,5-diyl) regiorandum (POT), high molecular weight poly(vinyl chloride) (PVC), tetrahydrofuran (THF, ≥ 99.5%), 2-hydroxy-2-methylpropiophenone (HMPP, > 97%), phenylbis(2,4,6-trimethylbenzoyl)phosphine oxide (PBPO, > 97%), 2,2-dimethoxy-2-phenylacetophenone (DMPP, > 99%), butyl-acrylate (>

99%), 1,6-hexanediol diacrylate (HDDA, 80%), and poly(propylene glycol) diacrylate (PPODA, M_n ~ 800) were purchased from Sigma-Aldrich (Dublin, Ireland). When possible, they were of selectophore grade or trace metal standard. N-decyl-methacrylate was obtained from Polysciences (Northampton, UK), 1,4-butanediol diacrylate (BDDA, > 99%) from Alfa Aesar (Heysham, UK), chloroform (> 99%) and ethanol (EtOH) from Fisher Scientific (Dublin, Ireland). 1-ethyl-3-methylimidazolium [emim][NTf_2], [emim] tris(pentafluoroethyl)trifluorophosphate, [FAP], 1-butyl-3-methylimidazolium [bmim][FAP] and 1-hexyl-3-methylimidazolium [hmim][FAP] were obtained from VWR (Dublin, Ireland). All chemicals were used as received. For the preparation of gaskets, 0.8 mm thick adhesive poly foam strips were purchased from Radionics (Dublin, Ireland). Deionised water with resistivity of 18.2 MΩ cm was obtained with a Milli-Q reagent-grade water system and it was used for making aqueous solutions.

2.2 Reference Electrode Preparation

Carbon screen printed electrodes, see Figure S1, were fabricated as described elsewhere [13]. POT and poly(3,4-ethylenedioxythiophene) (PEDOT) were deposited onto these electrodes to form the underlying mixed conductivity solid contact layer. The POT and EDOT solutions were stirred overnight and for ~1 hour, respectively, to facilitate solubilisation. The solid contact layer was prepared by drop-casting a total amount of 15 µL of 2.75 mg mL^{-1} POT chloroform solution onto the underlying carbon layer. Alternatively, PEDOT was electrochemically grown on the carbon electrodes from a 0.05 M EDOT solution in [emim][FAP] or [emim][NTf_2] which was stirred at 1000 rpm. During this process, the potential was scanned 25 times between 0 and 1.0 V with a scan rate of 50 mV s^{-1} or held at 1.0 V for 900 seconds. (Stirring of solution helped the formation of homogeneous, i.e., patch-free, film while electrodeposition without stirring resulted in PEDOT film formation mostly limited at the outer ring of the electroactive disk). At the end of the PEDOT deposition, the electrodes were rinsed with EtOH, followed by H_2O and again with EtOH. The electrodes were finally dried by blowing N_2 over them and stored in a covered petri dish.

For the preparation of the capping membranes, the IL was vortexed for ~1 hour with the acrylate monomer/s, the cross-linker and the photo-initiator. 9 µL of the resulting membrane liquid formulation was drop-cast onto the electrodeposited PEDOT layer within a 3.0 mm diameter well formed by punching a hole in an adhesive foam tape covering layer,

which was then fixed around the carbon disk. The acrylate solution was polymerized via a free radical initiated mechanism without flushing N_2, i.e., by 40 minutes irradiation under UV or white light, using the CL-1000 ultraviolet cross-linker UVP source, or the Dolan-Jenner Fiber-lite LMI-6000 lamp, respectively. Table S1 in the Supporting Information reports details of the membrane formulations screened in this investigation. For all the formulations the amount of photo-initiator and IL was 0.8 % and 6 % of the molar content of the acrylate monomer/s used, respectively. (Note: when combining monomers the molar ratio is referred to the sum of the molar content of the two monomers). Unless differently stated, all the percentages reported for the membrane components are given in respect to the molar content of the acrylate monomer/s. The membrane mixture was freshly prepared, carefully protected from direct sunlight and used within few hours of preparation. If not explicitly stated, the electrodes were conditioned overnight in aqueous 10 mM NaCl. Na^+-SC-ISEs electrodes were prepared in-house. The ISE solid-contact was a PEDOT layer potentiostatically deposited from [emim][NTf_2] as described above for the reference electrodes. The ISE capping membrane prepared as reported elsewhere [14] was a ionophore doped PVC formulation and was drop-cast on the PEDOT layer.

2.3 Instrumentation and Software. The potentiometric measurements were recorded using the EMF-16 voltmeter from Lawson Labs, USA. The potential of the above electrodes was measured against an in-house made silver/silver chloride (saturated KCl) and a double-junction Ag/AgCl (Sigma Aldrich, Ireland) during conditioning and testing, respectively. An Ag and a Pt wire were employed during the EDOT electro-polymerization as pseudo-reference and counter electrodes. CHI-900 (CH-instruments, USA) was used to carry out the electropolymerization of the conducting polymer on dual screen printed electrode substrates. A pH meter (SympHony SP70P) from VWR was used to check the pH of aqueous solutions and to validate pH measurements of sublingual saliva samples which were collected using a sterile pipette from volunteers. All the SEM images were captured with the Hitachi S3000N in the secondary electron mode using an accelerating voltage of 5 kV.

3. Results and Discussion

POT and PVC doped with ILs have been used previously [10] as the solid contact and capping membrane, respectively, for the preparation of SCI-REs. PVC has been the material of choice for decades in the preparation of ion-selective electrodes (ISEs) and, in

this respect, its use in reference electrodes is therefore understandable. However, polyacrylates have attractive qualities for electrodes with ionogel-based capping layers, such as lower levels of ionic contaminants [15] and a lower dielectric constant [16, 17] which reduces ion-exchange behaviour, and may enhance the retention of IL within the layer. The availability of various acrylate monomers, along with diverse cross-linkers and photo-initiators offers the possibility to create polymers with a wide range of physical and mechanical properties [15]. Besides, nonplasticised polyacrylates matrices are important in biomedical applications because of their biocompatibility and compatibility with thick- and thin-film microfabrication technologies [5, 6, 8]. With respect to the solid-contact layer, POT re-dissolves during the drop-casting of the PVC/IL capping membrane from a THF solution, as experimentally demonstrated in Figure S2. Preliminary tests with electrodes prepared with POT (SC) and PVC/IL (capping membrane) layers showed slow polarization of the potentiometric curves when the measurement was stopped and then re-started after few minutes, without removing the electrodes from the solution (results not shown). This slow polarization is probably an indication of a water layer building up at the internal interface, i.e., formation of a thin aqueous inner phase beneath the PVC capping membrane [18, 19]. While POT should impede the formation of a water-layer at the electrode/polymer interface because of its hydrophobicity, the above re-dissolution caused it to fail to fully cover the carbon surface thus contributing to the slow polarization curves observed with these electrodes.

For the above reasons, PEDOT electrochemically deposited from IL-media and polyacrylates based ionogels were investigated as solid-contact and capping membrane materials, respectively. In regard to the capping membrane, the [FAP] anion ILs family was chosen for their low water solubility. For instance, the mole fraction aqueous solubilities of [hmim][NTf_2] and [hmim][FAP] are 10^{-4} and ~ 10^{-6} [20-24] respectively, which raises the possibility of a significantly larger leaching rate of the IL from the membrane in the former case. Leaching may not only impact on the stability of the electrode potential but it may also be hazardous in certain circumstances, e.g., environmental or wearable applications. A range of acrylate formulations containing equal amount of IL ([emim][FAP], 6 %), cross-linker (HDDA, 3.0 %) and photo-initiator (DMPP, 0.8%) was tested as listed in Table S1. It was found that highly uniform membranes with rubbery (but not tacky) character could be obtained by polymerizing a mixture of butylacrylate and N-decylmethacrylate in the ratio 9:1. In contrast, polymerization of butyl-acrylate alone resulted in a more wrinkly gel. In case of N-decylmethacrylate alone or 1:1 mixtures of butylacrylate and N-decylmethacrylate

the resulting polymers tended to be too soft/runny in nature. The level of cross-linker in the co-monomers mixture was also found to have a significant effect on the resulting polymer characteristics. Therefore, an optimization processes was employed starting from a base mixture of butylacrylate and N-decylmethacrylate in the ratio 9:1, and varying the composition in a systematic manner. For example, the amount of HDDA was increased from 1.5% through 3.0% to 4.5% in steps of 1.5%, and the optimal was found to be around 3.0%, because the corresponding membranes produced using 1.5 % and 4.5 % HDDA in the monomers formulation were respectively too sticky or too stiff to be of practical use for our application.

Figure 1 shows the results obtained with membranes based on poly(butyl-co-decylmethacrylate) containing various cross-linkers, photo-initiators and types of solid-contact. Several conclusions can be drawn from these results. Firstly, all of the membranes exhibited moderate cation-exchange behaviour, but they were quite insensitive to variations of sample pH over the range pH 4-7. This would suggest that [FAP] acted as a cation-exchanger site in the membrane to a certain extent because the potential of electrodes immersed in a 0.1 M KCl solution was always higher in comparison to the same electrodes immersed 0.1 M NaCl solution. Secondly, the figure demonstrates that the use of PBPO instead of DMPP as photo-initiator increased the sensitivity of the electrodes towards Na^+ and K^+. With ionogels formed using PBPO (– · –), the electrode potential increased by ~35 mV and by ~40 mV when the NaCl and KCl concentrations increased from 1 mM to 0.1 M, respectively. For equivalent ionogels formed using DMPP (– –), the electrode potential increased less, i.e., 18.5 ± 1.9 mV and 30.5 ± 8.7 mV (n=4). This difference may arise from the presence of residual photo-initiator and its by-products in the membrane, as these are known to exhibit ion-exchange behaviour [25]. Thirdly, electrodes with membranes produced using PPODA (· · ·) as cross-linker showed larger sensitivity towards Na^+ and K^+ than equivalent membranes produced using HDDA (– –). For example, electrodes based on these membranes showed shifts in potential of the order of ~50 and ~60 mV, respectively, when the Na^+ and K^+ concentrations were raised from 1 mM to 0.1 M. HMPP was discarded as photo-initiator as it was found to produce very stiff and thin membranes that tended to peel away from the underlying layers. HDDA[1] and DMPP were therefore selected

[1] BDDA, which has a $-(CH_2)_4-$ chain rather than the $-(CH_2)_6-$ group present in HDDA, produced membranes with almost identical behaviour (results not shown).

as cross-linker and photo-initiator, respectively, while PPODA and PBPO were discarded from further investigation.

The redox state of the conducting polymer appears to affect the electrode potential during conditioning, as shown in Figure 2. The level of doping in the polymer should be different depending on the deposition technique employed, i.e., PEDOT deposited using CV should be in a less oxidised state [26] than the potentiostatically deposited polymer. The latter fact occurs because the potential was reversed back to 0.0 V or it was held at 1.0 V (corresponding to the onset of the oxidation of the monomer) in case of CV or potentiostatic deposition, respectively. In Figure 2, for the CV-generated SC-layer, the potential of the resulting electrodes increased sharply for the first 2.5 hours during conditioning, at a rate of ca. 0.80-0.90 mV min^{-1}, and then levelled off during the final 5 hours, with a typical final drift of 3.5-4.5 mV h^{-1}. However, equivalent electrodes prepared using potentiostatically generated PEDOT SC-layer showed significantly different behaviour. After a much smaller increase of ca. 15-20 mV during the initial 1.5 hours, the potential levelled off with a typical drift of -0.01 mV h^{-1} during the final 5 hours.

This finding seems in agreement with the spontaneous oxidation of the PEDOT SC-layer accompanied by the relative ion fluxes at the SC/membrane and membrane/sample interfaces to maintain the overall electro-neutrality within the electrode layers, see Scheme I. Significantly, Michalska and Maksymiuk [27] demonstrated that spontaneous charging/discharging may occur at the SC-layer underlying a polymeric ion-selective membrane affecting the response pattern of the sensor. However, it should be also noted that the morphology of the PEDOT layer was significantly different depending on the deposition method, as shown in Figure 3a and 3b. The polymer had web-like structures or a globular film-like appearance when deposited by potentiostatic polarization or by CV, respectively. In this regard, it is significant that Paczosa-Bator et al. [28] observed that PEDOT films doped with triphosphate to bind Mg^{2+} and Ca^{2+} prepared by dynamic polarization were smoother and denser that the ones prepared by potentiostatic deposition. In addition, the authors showed that the smoother films resulted in faster potentiometric responses although sensitivities values were similar in both cases. Therefore, further experiments are needed to understand more clearly the impact of the CP redox state on the overall electrode response.

In order to prepare electrodes with behaviour closer to that of an ideal reference electrode, the above results underline the need to optimise multiple aspects of the device fabrication,

such as the media used for electropolymerization of the CP and the type of IL present in the membrane. Figure 4 demonstrates the effect of ILs in the membrane formulation for electrodes having a potentiostatic grown PEDOT SC-layer. In fact, replacing [emim][FAP] (· · ·) with [hmim][FAP] (—) produced a smaller variation in the potential of the electrodes when these were in contact with different electrolyte solutions. For [hmim][FAP], when NaCl and KCl concentrations were increased from 1 mM to 0.1 M, the electrode potential increased by 5 ± 1 mV and by 15 ± 2 mV (n= 4, and excluding the initial 2-3 minutes after swapping solutions), respectively.

It is interesting to note that, as shown in Figure S3, the choice of IL impacted also on the dynamics of the electrode potential during the conditioning step. During the first 2.5 hours of conditioning, the potential increased in all the three cases, in the order [emim] > [bmim] > [hmim]. Then the potential tended to level off and typical drifts experienced during the last 10 hours of testing were 0.9–1.1 mV h^{-1}, 0.2–0.4 mV h^{-1}, -(1.5–1.8) mV h^{-1}, respectively, for ionogel membranes based on [emim], [bmim] and [hmim]. Thus, it seems that by selecting more hydrophobic IL cations, the initial rise in the potential can be reduced. This observation seems also to be in agreement with Scheme I, as, since bulkier ions will tend to partition less into the aqueous phase, the CP layer would be affected to a lesser extent, and the electrode reaches the "equilibration" potential more rapidly.

Regarding the effect of the CP redox state, it is significant to note that previous reports have highlighted the crucial role of charging/discharging processes of the conducting polymer at the potentiometric detection limit of SC-ISEs [27]. Less obviously, the media used for the CP electro-polymerization may impact on the doping/de-doping of the CP since this process depends on the anions incorporated in the polymer skeleton backbone [29, 30]. Therefore the polymerization of EDOT was conducted in [emim][NTf_2] instead than [emim][FAP], as employed above, and it was found that the electro-deposition proceeded very differently. With [emim][FAP], an orange colour appeared in the IL proximal to the working electrode, while for the equivalent experiment with [emim][NTf_2], the IL remained transparent. In addition, PEDOT electrodeposited from [emim][NTf_2] by CV resulted in partial coverage of the carbon layer, as shown in the SEM picture in Figure S4. Figure S5 shows that typically the current and the total charge passed in the oxidative region, and therefore the amount of material deposited, tended to be larger in the CVs recorded in [emim][FAP] than in [emim][NTf_2]. As less material is deposited with [emim][NTf_2], this will lead to thinner layers and may explain the incomplete coverage of the substrate under the same electrochemical deposition technique. Under potentiostically controlled conditions in the

same IL, i.e., [emim][NTf_2], a homogenous layer of PEDOT was obtained with 'cauliflower'-like surface nodules, see Figure 5. This different surface topography may arise from the fact that the viscosity and conductivity of [emim][FAP], i.e., 75 cP and 3.6 mS cm^{-1} [31], differ significantly from [emim][NTf_2], i.e., 32 cP and 9.1 mS cm^{-1} [32]. For instance, the larger viscosity of [emim][FAP] would inhibit monomer diffusion towards the electrode, and therefore polymer growth will be slower in this IL (under diffusion controlled regime) because of the smaller diffusion coefficient¸ D_i, as given by the Stokes-Einstein equation [33]:

$$D_i = \frac{k_B T}{6\pi\eta r_i}$$

where k_B, T, η, and r_i are the Boltzmann constant, the absolute temperature, the viscosity of the solution and the radius of the chemical species i, respectively. According to the above equation and the given viscosity values, the diffusion coefficient in [emim][NTf_2] is 2.3 time larger than what would be in [emim][FAP]. In addition, the role of the IL anion acting as a template during the polymerization cannot be excluded as origin of the morphological difference of the PEDOT layers obtained from the two ILs. For instance, Ahmad et al. [34, 35] showed that 1-ethyl-3-methylimidazolium bis(perfluoroethylsulfonyl)imide assisted the growth of PEDOT in a fibre-type form.

Figure 6a and 6b show results of immersion tests obtained with electrodes, after conditioning in aqueous 10 mM NaCl overnight or for 2 hours (see Figure S6 for the potential profile during the conditioning step). In both Figure 6a and 6b, the SC was PEDOT potentiostatically deposited from a [emim][NTf_2] solution, and capping membranes are based on [bmim][FAP] and [hmim][FAP]. It is interesting to note that in Figure S6, during the last 10 hours of the longer conditioning step, the electrode potential drifted by -(1.0–2.0) mV h^{-1} and -(3.0–6.0) mV h^{-1}, respectively, for membranes containing [bmim][FAP] and [hmim][FAP]. These values are larger than those observed with electrodes that had same capping membrane but had the PEDOT SC-layer potentiostatically deposited from [emim][FAP], i.e., -(0.2–0.4) mV h^{-1} and -(1.5–1.8) mV h^{-1} respectively. More importantly, electrodes in Figure 6a, which were conditioned overnight, showed a steadily increasing response upon initial contact with 1 mM NaCl solution. When the conditioning step was stopped after 2 hours, i.e., at a plateau in the potential response curve and before the start of the drift, for both ionogels, the electrodes showed more stable responses. In fact, in Figure 6b, the potential increased by 5.5 ± 1.0 mV and 10.5 ± 1.3 mV for [hmim][FAP] and by 4.5 ± 0.6 mV and 14.2 ± 0.3 mV for [bmim][FAP] (n=4 and

excluding the initial 3-5 minutes after contacting the test solution) when the concentration was increased from 1 mM to 0.1 M, for NaCl and KCl, respectively. Overall, the best performing capping membranes were based on a 9:1 butylacrylate/decyl-methacrylate mixture containing 0.8 % DMPP, 3% HDDA and 6 % [hmim][FAP]. Regarding the SC-layer, PEDOT films were potentiostatically grown from [emim][FAP] or from [emim][NTf_2], and electrodes conditioned overnight or for 2 hours, respectively.

Besides minimizing the offset of the electrode potential in response to sample solutions having different composition, assuring high batch reproducibility is another key requirement to deliver low-cost reference electrodes. In fact, these electrodes should present an inter-electrode offset ideally in the order of few mV. This requirement would assure that individual calibration is not needed but instead the whole batch can be calibrated by averaging the offset (against a standard reference electrode) of a statistical significant portion of the lot. Perhaps, batch reproducibility is one of the major limitations affecting this new class of reference electrode based on ionogels. Figure 7 presents a comparison of 4 electrodes prepared according to the optimized procedure described above. In fact, all these electrodes have the same capping membrane (based on a 9:1 butylacrylate/decyl-methacrylate mixture containing 0.8 % DMPP, 3% HDDA and 6 % [hmim][FAP]), the same SC-layer (a PEDOT film potentiostatically deposited from [emim][NTf_2]) and they were conditioned for 2 hours. However, the PEDOT layer was left ageing for a week and for 6 weeks after its electrodeposition prior depositing the capping membrane. The figure suggests that electrodes belonging to the same batch have very similar trends (within ± 5 mV) when tested with solutions of different composition although more accurate conclusions would require a more significant statistical sample. In addition, this figure seems to highlight that PEDOT ageing (and perhaps its de-doping) impact significantly on the offset of the electrodes.

The best-performing SCI-REs were further assessed to evaluate their potential stability in real-saliva samples while changing the pH of the sample by adding dropwise 0.1 M HCl. Figure 8 shows that the potential of the SCI-RE was quite stable, i.e., average and standard deviation equal to 273.4 and 4.2 mV, respectively, while the pH of the saliva sample was changed from 7 to 4.1. In addition, the SCI-REs were also assessed as reference electrodes in a potentiometric calibration experiment using Na^+-SC-ISE fabricated in-house. Figure 9 compares the calibration curves of three different Na^+-SC-ISE obtained using the optimized SCI-RE, and a conventional double-liquid junction Ag/AgCl. From these calibration curves the slope was found to be 56.9 mV/log a_{Na^+} and 56.7 mV/log a_{Na^+}, respectively. The small

difference in the two slope values means that the two calibration curves overlap almost perfectly when the offset (due to the gap in the potential between the Ag/AgCl and SCI-RE electrodes, ca. 408 mV) is zeroed. These results showed that the combination of a Na^+-SC-ISE and a SCI-RE on the same screen printed substrate can be used to realize low-cost, disposable potentiometric strips. The two electrodes have a common SC layer, which is convenient for mass-production since this design offers flexibility in terms of electrode size and form factor. The only difference lies in the final capping membrane. This configuration opens up new potential applications for which glass bodied electrodes or large conventional designs are unsuitable. For example, the use of these for on-body sweat sensing using patch-type configurations will be presented in a future communication.

Conclusions

This work describes the preparation of disposable reference electrodes based on a PEDOT solid-contact layer and an ionogel capping membrane realized by incorporating ILs within polyacrylate polymerized *in situ*. The potential of this novel reference electrode monitored against a commercial Ag/AgCl while contacting a real-saliva sample seems stable over short times and to pH changes induced by addition of an acid solution. In addition, the reference electrode was employed in combination with Na^+-SC-ISEs for potentiometric calibration of solutions with increasing sodium concentrations. Calibration curves obtained with the above reference electrode overlap with those obtained using a double-junction Ag/AgCl as reference electrode once of the offset between the two is zeroed. Future research will address the integration of these electrodes in wearable potentiometric strips for the analysis of accessible body fluids.

Acknowledgments

Science Foundation Ireland is gratefully acknowledged for supporting this project under the CLARITY CSET award 07/CE/I1147.

FIGURES and CAPTIONS

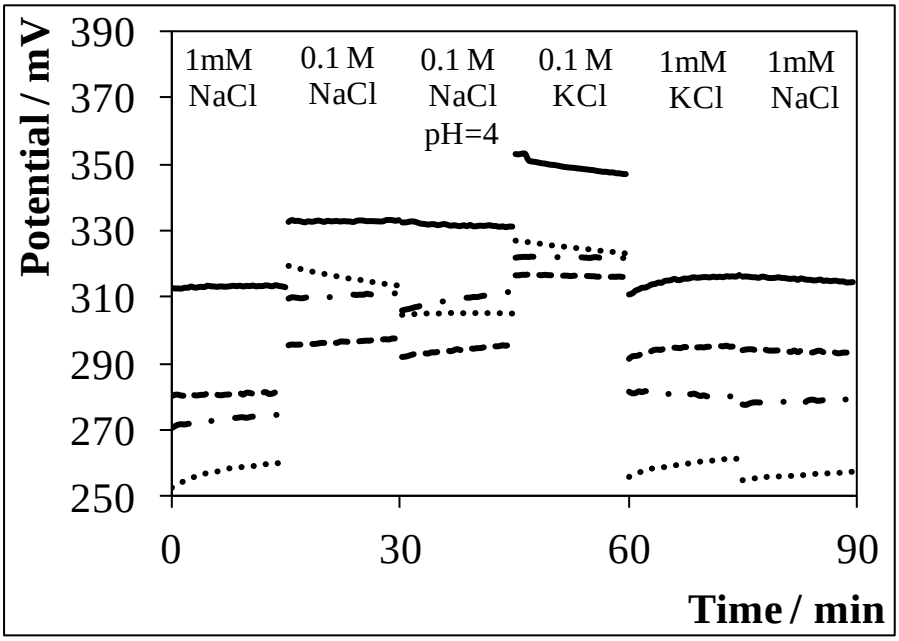

Figure 1. Individual responses of reference electrodes prepared by entrapping [emim][FAP] within a poly(butyl-co-decylmethacrylate) membrane polymerized *in situ*. Three electrodes have a PEDOT solid-contact layer electrodeposited by CVs from [emim][FAP], and their membranes contained: 3 % (– –) HDDA or (· · ·) PPODA as cross-linker together with 0.8 % of DMPP as photo-initiator, or (– · –) 3 % HDDA together with 0.8 % of PBPO as photo-initiator. In one case (—), the PEDOT solid-contact layer was electrodeposited potentiostatically from [emim][FAP] and the membrane contained: 3% HDDA and 0.8 % DMPP. The electrode potential was recorded over 15 minutes for each bathing solution, as labelled in the figure.

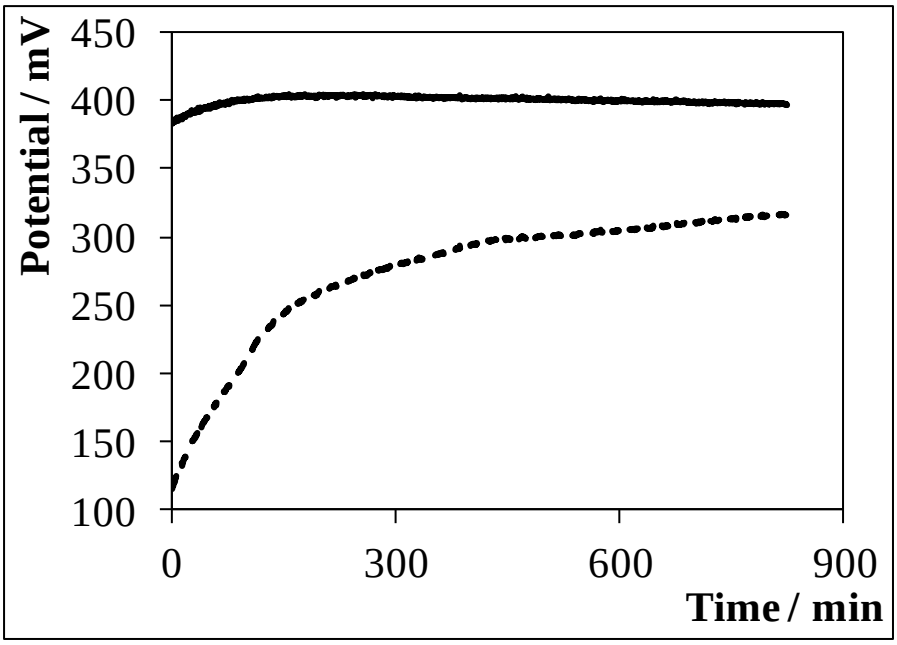

Figure 2. Conditioning step of reference electrodes prepared by entrapping [emim][FAP] in a poly(butyl-co-decylmethacrylate) membrane while in contact with a 10 mM NaCl solution. The solid-contact consisted of PEDOT deposited from a 50 mM EDOT solution in [emim][FAP] by (—) potentiostatic and (– –) CV polarization.

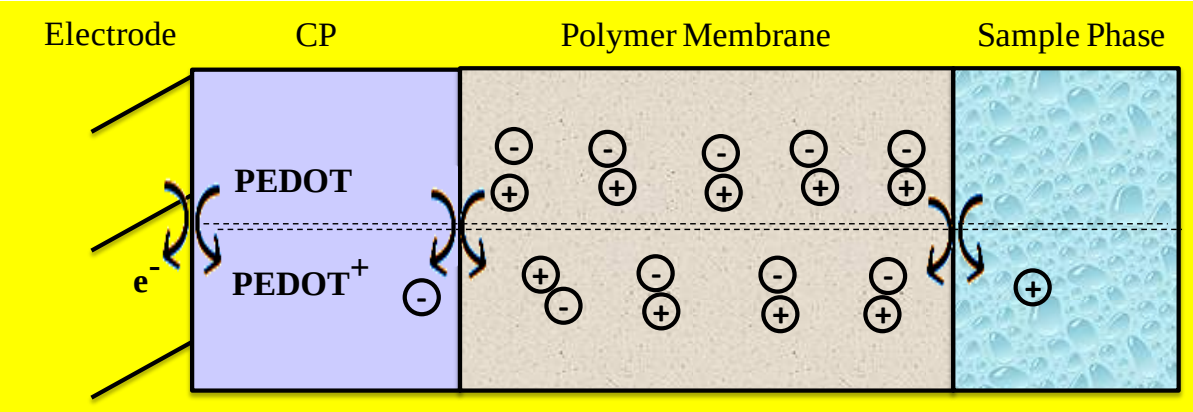

Scheme I. The schematic representation of the ion-fluxes at the SC-bulk membrane and at the bulk membrane-sample interfaces for a membrane loaded with an IL constituting of cations and anions. The ion-fluxes are accompanied by the spontaneous oxidation processes of the PEDOT layer at the SC-electrode interface leading from the scenario depicted above the double dashed line to the situation illustrated below this mark.

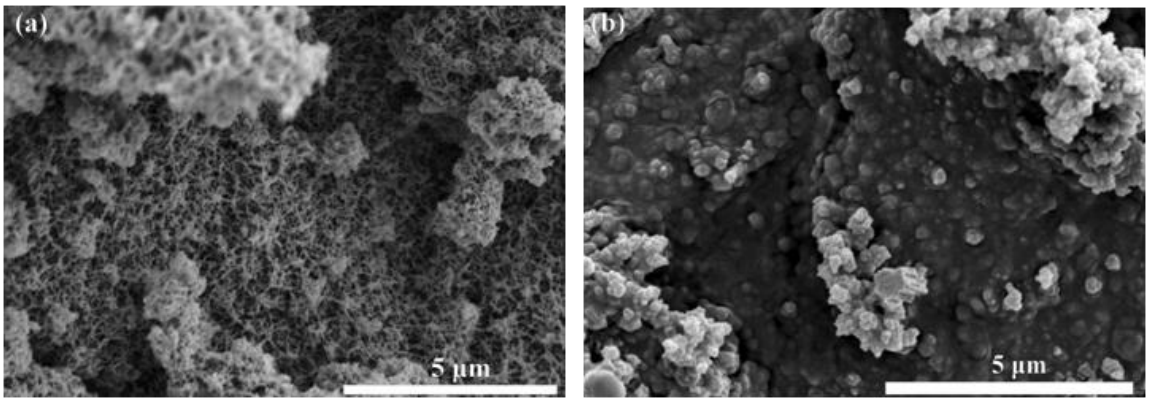

Figure 3. SEM images of PEDOT electrodeposited from [emim][FAP] (a) potentiostatically, at 1.0 V, and (b) by cycling the potential 25 times between 0 and 1.0 V with scan rate of 50 mV s^{-1}.

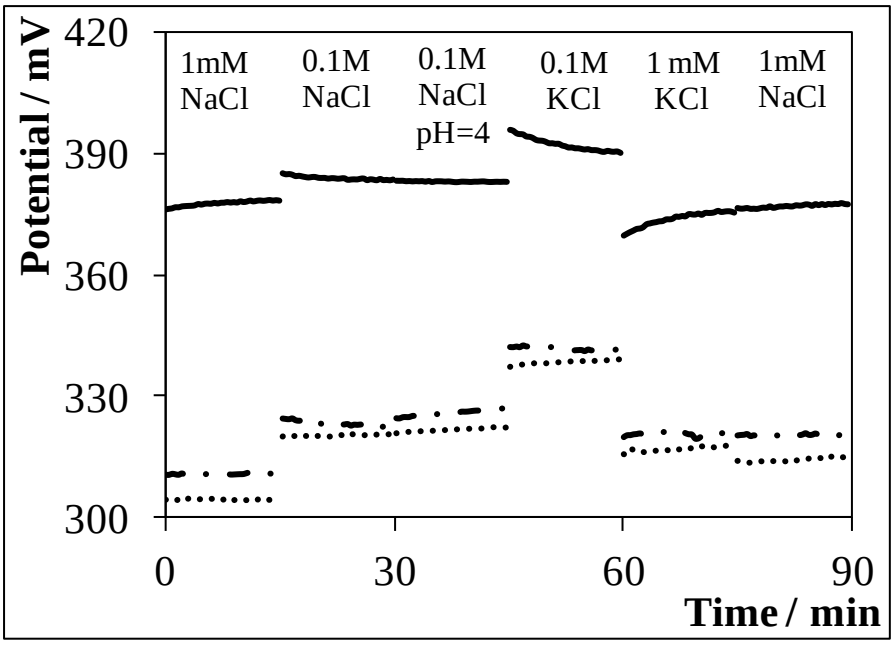

Figure 4. Individual responses of reference electrodes prepared by entrapping (—) [hmim][FAP], (– · –) [bmim][FAP] or (· · ·) [emim][FAP] within a poly(butyl-co-decylmethacrylate membrane. The solid-contact was a PEDOT layer potentiostatically electrodeposited from [emim][FAP]. The electrode potential was recorded over 15 minutes for each bathing solution, as labelled in the figure.

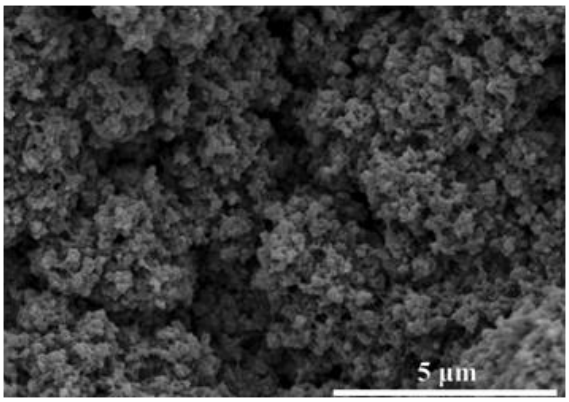

Figure 5. SEM image of PEDOT electrodeposited from [emim][NTf_2] by applying a constant potential of 1.0 V vs. Ag wire for 900 seconds.

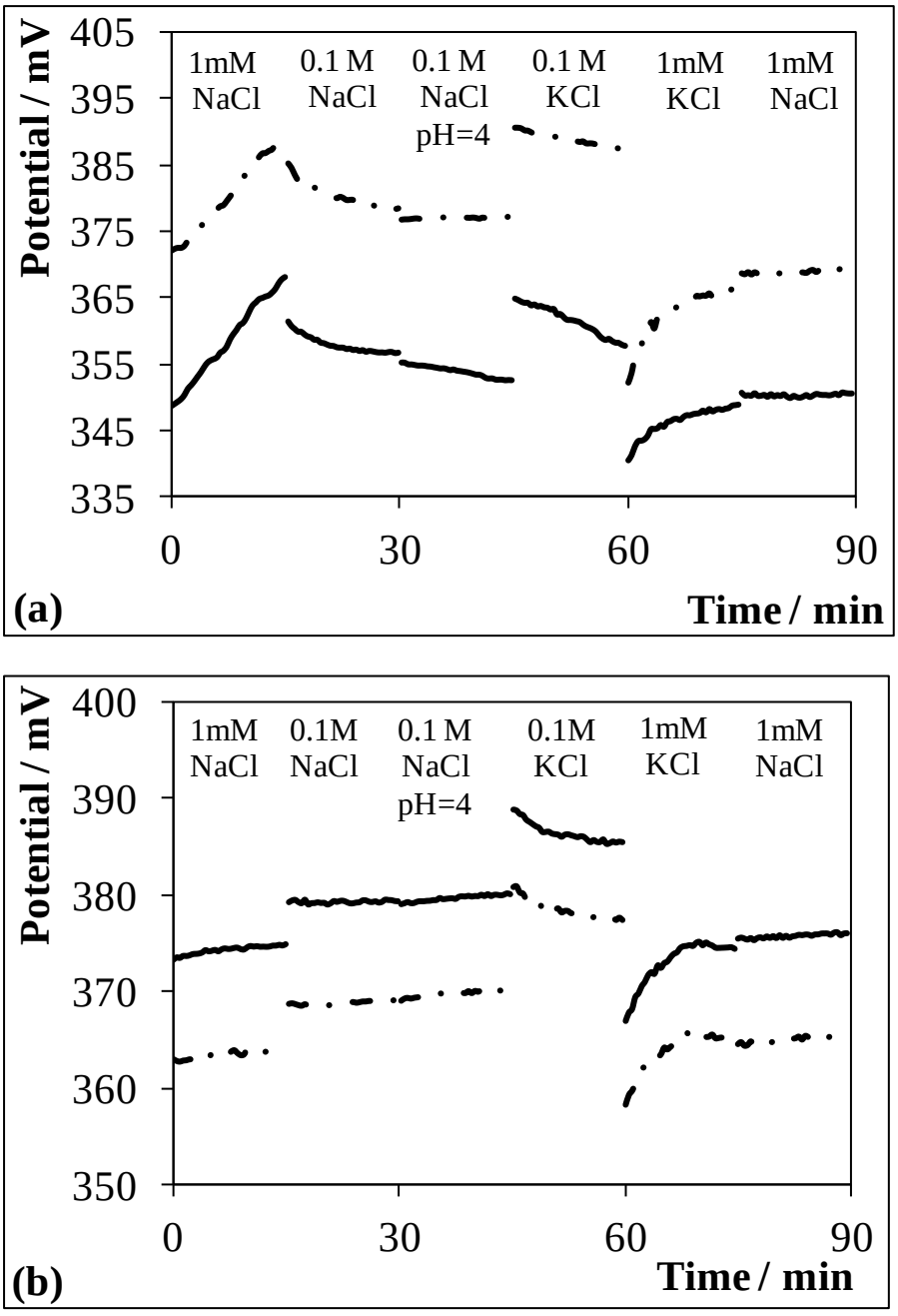

Figure 6. Individual responses of reference electrodes prepared by entrapping (—) [hmim][FAP] and (– · –) [bmim][FAP] within a poly(butyl-co-decylmethacrylate) membrane. The solid-contact was a PEDOT layer potentiostatically electrodeposited from [emim][NTf_2]. The electrode potential was recorded over 15 minutes for each bathing solution, as labelled in the figure, after (a) overnight and (b) 2 hours conditioning in aqueous 10 mM NaCl.

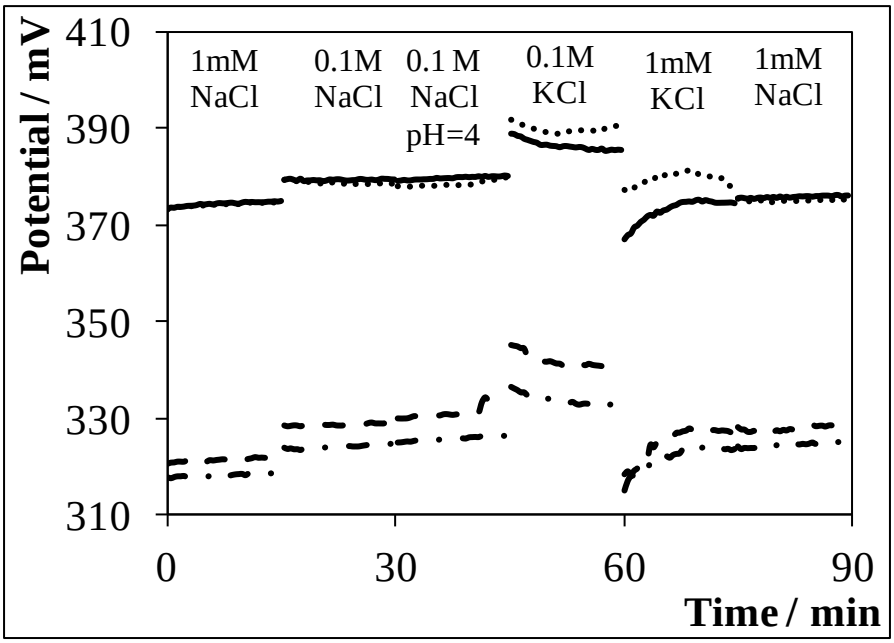

Figure 7. Individual responses of reference electrodes prepared by entrapping [hmim][FAP] within a poly(butyl-co-decylmethacrylate) membrane polymerized *in situ*. The solid-contact was a PEDOT layer potentiostatically electrodeposited from [emim][NTf_2] which was aged for 1 week (—) (· · ·) and for 6 weeks (– –) (– · –). The electrode potential was recorded over 15 minutes for each bathing solution, as labelled in the figure.

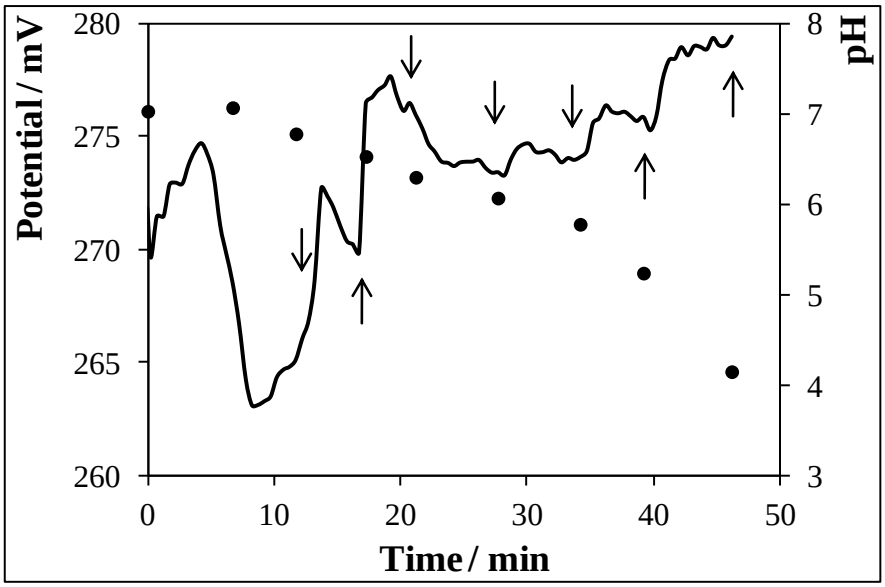

Figure 8. (—) Trend of the potential of an SCI-RE against a Ag/AgCl reference electrode while contacting a real-saliva sample. The pH of the saliva sample was changed by adding dropwise 0.1 M HCl. (●) Measurements of the saliva sample pH as determined using a pH-meter after 1 minute stabilization following the addition of an aliquot of 0.1 M HCl at the times indicated by the arrows. The SCI-RE had a PEDOT SC-layer potentiostatically deposited from [emim][FAP] and capping membrane loaded with [hmim][FAP].

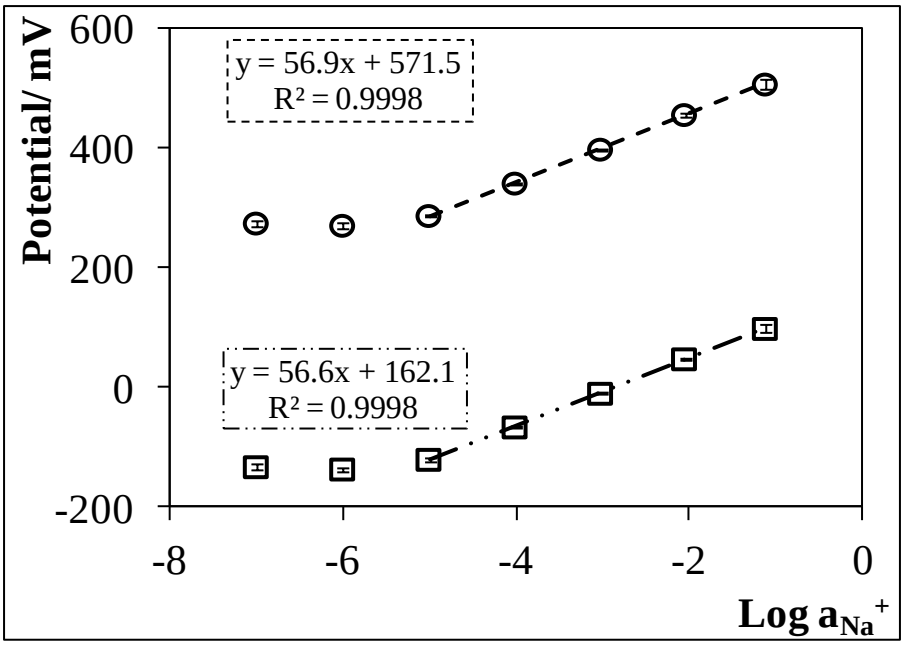

Figure 9. Average of calibration curves for three Na^+-SC-ISE against (○) a double-liquid junction Ag/AgCl reference electrode and (□) the optimized SCI-RE which had a PEDOT SC-layer potentiostatically deposited from [emim][NTf_2] and capping membrane loaded with [hmim][FAP]. Error bars indicate the standard deviation.

Supporting Information

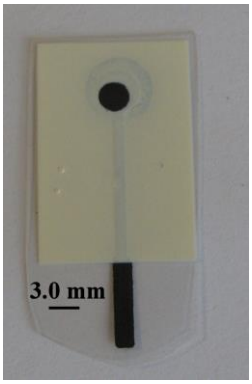

Figure S1. Picture of a screen printed carbon electrode.

Table S1. Membrane formulation specifying acrylate monomer/s, crosslinker, photo-initiator, IL and the appearance of the resulting membrane. The percentage values reported for the crosslinker, photo-initiator and IL are given in respect to the molar content of the acrylate monomer/s (monomer or sum of the monomers equal to 3.57 mmoles).

Monomer/s	Cross-linker	Photo-initiator	IL	Appearance
Butylacrylate / 512.0 µL	HDDA / 24.0 µL (3.0%)	DMPP / 7.3 mg (0.8%)	[emim][FAP] / 69.0 µL (6.0%)	Wrinkly
Decylmethacrylate / 461.0 µL	HDDA / 12.0 µL (3.0%)	DMPP / 3.6 mg (0.8%)	[emim][FAP] / 34.5 µL (6.0%)	Runny
Butylacrylate / 256.0 µL Decylmethacrylate / 461.0 µL	HDDA / 24.0 µL (3.0 %)	DMPP / 7.3 mg (0.8%)	[emim][FAP] / 69.0 µL (6.0%)	Runny
Butylacrylate / 461.0 µL Decylmethacrylate / 92.3 µL	HDDA / 24.0 µL (3.0%)	DMPP / 7.3 mg (0.8%)	[emim][FAP] / 69.0 µL (6.0%)	Rubbery
Butylacrylate / 461.0 µL Decylmethacrylate / 92.3 µL	HDDA / 12.0 µL (1.5%)	DMPP / 7.3 mg (0.8%)	[emim][FAP] / 69.0 µL (6.0%)	Rubbery/Soft
Butylacrylate / 461.0 µL Decylmethacrylate / 92.3 µL	HDDA / 36.0 µL (4.5%)	DMPP / 7.3 mg (0.8%)	[emim][FAP] / 69.0 µL (6.0%)	Rubbery/Stiff
Butylacrylate / 461.0 µL Decylmethacrylate / 92.3 µL	BDDA / 19.6 µL (3.0%)	DMPP / 7.3 mg (0.8%)	[emim][FAP] / 69.0 µL (6.0%)	Rubbery
Butylacrylate / 461.0 µL Decylmethacrylate / 92.3 µL	HDDA / 24.0 µL (3.0%)	PBPO / 12.0 mg (0.8%)	[emim][FAP] / 69.0 µL (6.0%)	Rubbery
Butylacrylate / 461.0 µL Decylmethacrylate / 92.3 µL	PPODA / 91.2 µL (3.0%)	DMPP / 7.3 mg (0.8%)	[emim][FAP] / 69.0 µL (6.0%)	Rubbery
Butylacrylate / 461.0 µL Decylmethacrylate / 92.3 µL	HDDA / 24 µL (3.0%)	HMPP / 12.0 mg (0.8%)	[emim][FAP] / 69.0 µL (6.0%)	Very Stiff
Butylacrylate / 461.0 µL Decylmethacrylate / 92.3 µL	HDDA / 24.0 µL (3.0%)	DMPP / 7.3 mg (0.8%)	[bmim][FAP] / 76.5 µL (6.0%)	Rubbery
Butylacrylate / 461.0 µL Decylmethacrylate / 92.3 µL	HDDA / 24.0 µL (3.0%)	DMPP / 7.3 mg (0.8%)	[hmim][FAP] / 83.6 µL (6.0%)	Rubbery

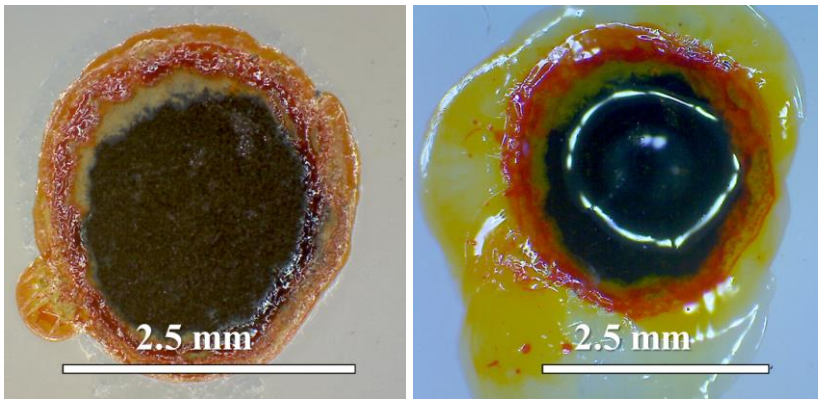

Figure S2. Photograph of the sensitive carbon area covered by POT (left) and after drop-casting a PVC/IL mixture solubilised in THF (right).

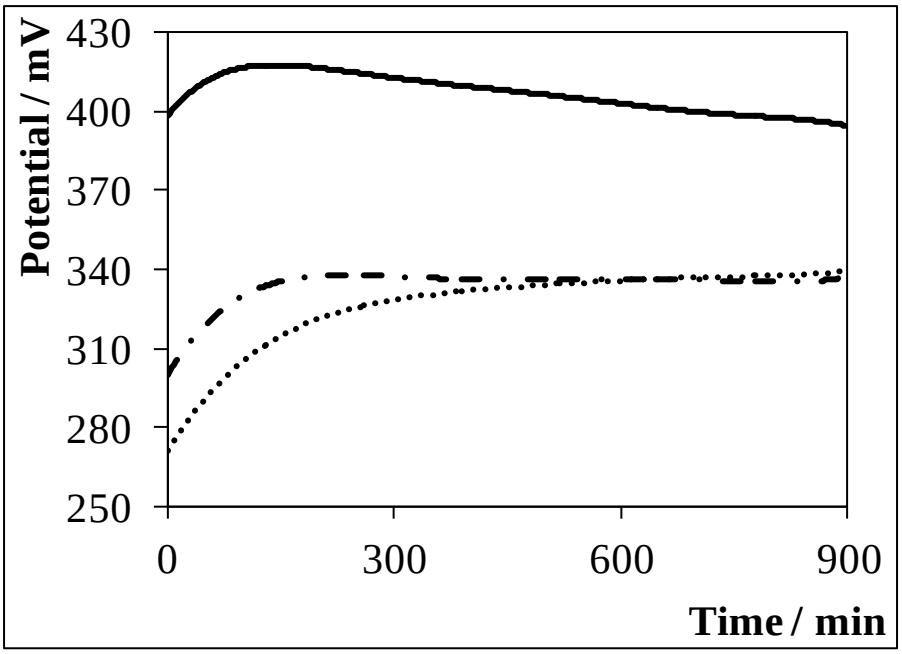

Figure S3. Conditioning step of reference electrodes prepared by entrapping (—) [hmim][FAP], (– · –) [bmim][FAP] or (· · ·) [emim][FAP] within a poly(butyl-co-decylmethacrylate) membrane. The conditioning solution was 10 mM NaCl while the solid-contact was a PEDOT layer potentiostatically electrodeposited from [emim][FAP].

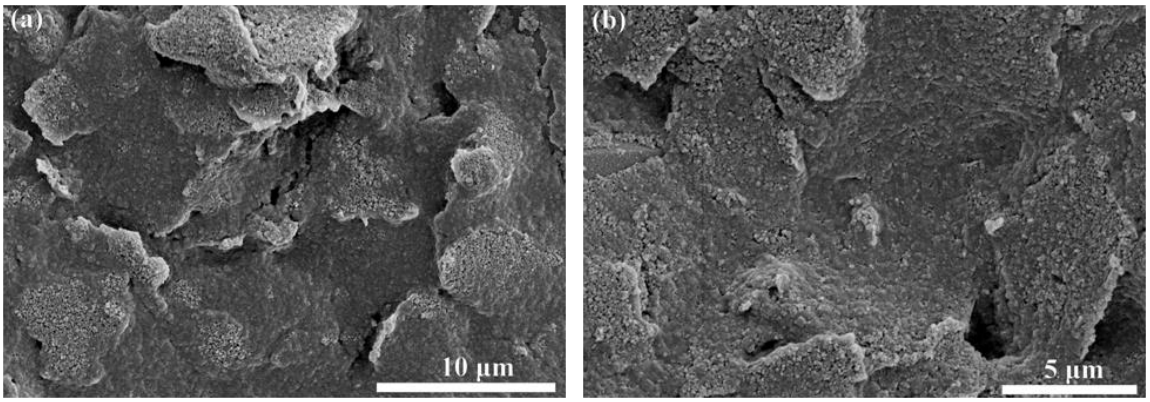

Figure S4. SEM images of PEDOT electrodeposited from [emim][NTf_2] by cycling the potential between 0 and 1.0 V vs. Ag wire for 25 times with a scan rate equal to 50 mV s^{-1}.

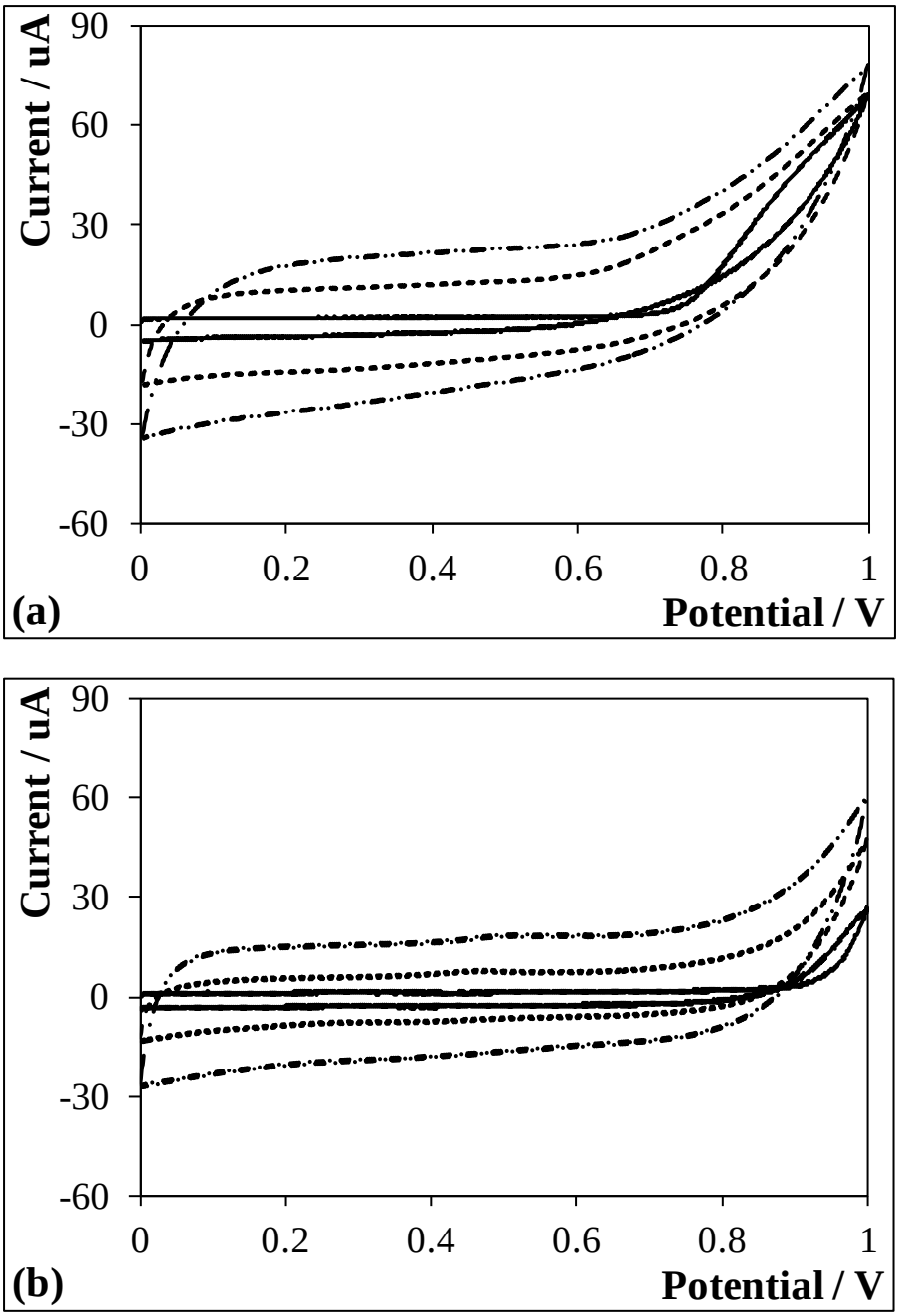

Figure S5. Electrodeposition of EDOT from a 50 mM solution in (a) [emim][FAP] and (b) [emim][NTf_2]. The traces show the (—) 1st, (– –) 10th and the (– · · –) 25th polymerization cycles.

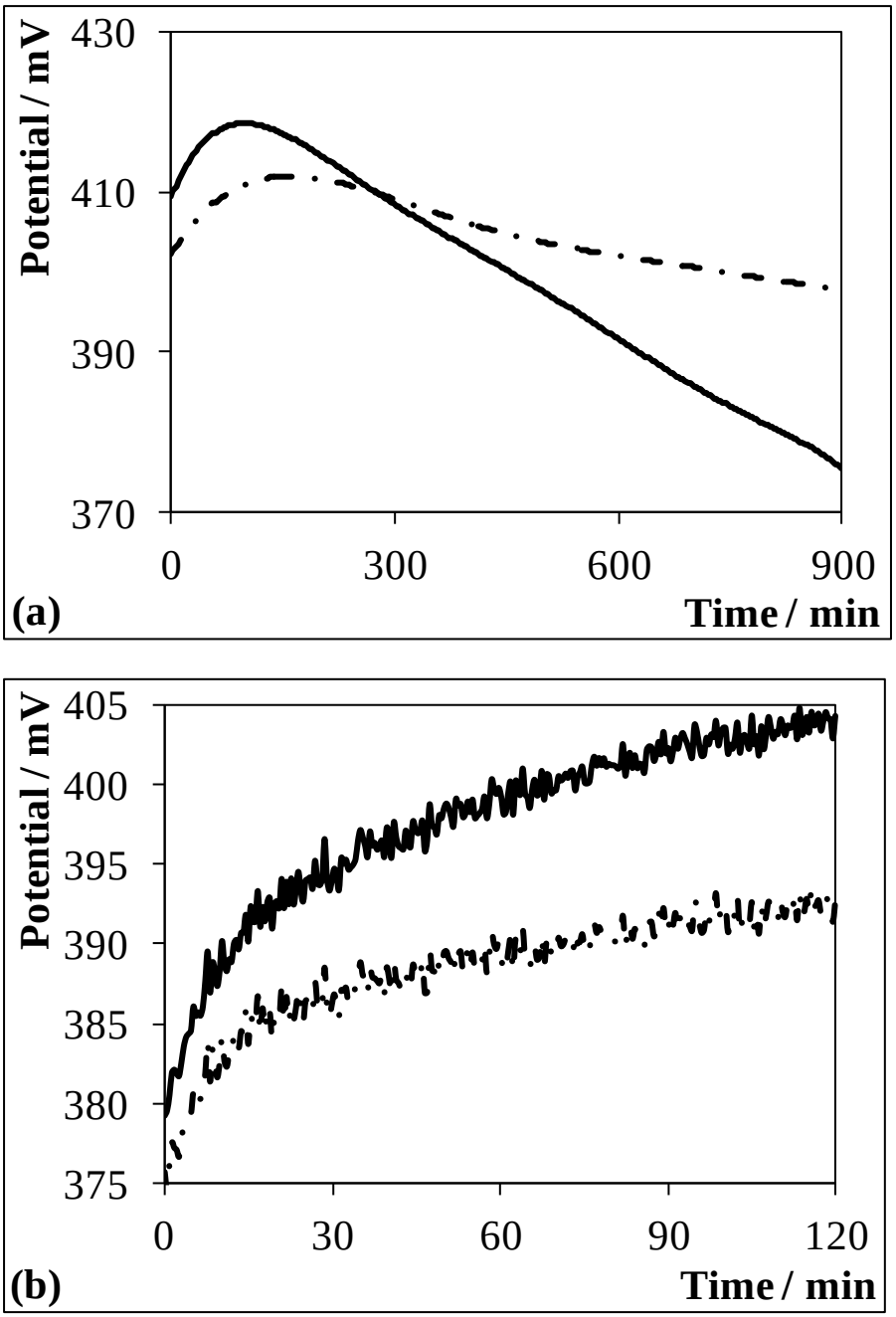

Figure S6. Conditioning step of reference electrodes prepared by entrapping (—) [hmim][FAP] and (– · –) [bmim][FAP] within a poly(butyl-co-decylmethacrylate) membrane. The solid-contact was a PEDOT layer potentiostatically deposited from [emim][NTf_2]. The electrodes were conditioned in aqueous 10 mM NaCl (a) overnight and (b) for 2 hours.

REFERENCES

[1] A. Michalska, Electroanalysis 24 (2012) 1253-1265.
[2] C. Zuliani, D. Diamond, Electrochimica Acta, 84 (2012) 29-34.
[3] U. Guth, F. Gerlach, M. Decker, W. Oelßner, W. Vonau, Journal of Solid State Electrochemistry, 13 (2009) 27-39.
[4] T.T. Zhang, C.Z. Lai, M.A. Fierke, A. Stein, P. Buhlmann, Analytical Chemistry, 84 (2012) 7771-7778.
[5] Z. Mousavi, K. Granholm, T. Sokalski, A. Lewenstam, Analyst, 138 (2013) 5216-5220.
[6] R.E. Dohner, D. Wegmann, W.E. Morf, W. Simon, Analytical Chemistry, 58 (1986) 2585-2589.
[7] Y. Mi, S. Mathison, E. Bakker, Electrochemical and solid state letters, 2 (1999) 198-200.
[8] R. Mamińska, A. Dybko, W. Wróblewski, Sensors and Actuators B: Chemical, 115 (2006) 552-557.
[9] T. Kakiuchi, T. Yoshimatsu, N. Nishi, Analytical Chemistry, 79 (2007) 7187-7191.
[10] D. Cicmil, S. Anastasova, A. Kavanagh, D. Diamond, U. Mattinen, J. Bobacka, A. Lewenstam, A. Radu, Electroanalysis, 23 (2011) 1881-1890.
[11] U. Mattinen, J. Bobacka, A. Lewenstam, Electroanalysis, 21 (2009) 1955-1960.
[12] S. Anastasova, A. Radu, G. Matzeu, C. Zuliani, D. Diamond, U. Mattinen, J. Bobacka, Electrochimica Acta, 73 (2012) 93-97.
[13] C. Zuliani, G. Matzeu, D. Diamond, Electrochimica Acta, (Submitted to Electrochimica Acta).
[14] B. Schazmann, D. Morris, C. Slater, S. Beirne, C. Fay, R. Reuveny, N. Moyna, D. Diamond, Analytical Methods, 2 (2010) 342-348.
[15] Y. Qin, S. Peper, E. Bakker, Electroanalysis, 14 (2002) 1375-1381.
[16] G. Lisak, E. Grygolowicz-Pawlak, M. Mazurkiewicz, E. Malinowska, T. Sokalski, J. Bobacka, A. Lewenstam, Microchim Acta, 164 (2009) 293-297.
[17] J.-P. Veder, R. De Marco, G. Clarke, R. Chester, A. Nelson, K. Prince, E. Pretsch, E. Bakker, Analytical Chemistry, 80 (2008) 6731-6740.
[18] T. Lindfors, L. Höfler, G. Jágerszki, R.E. Gyurcsányi, Analytical Chemistry, 83 (2011) 4902-4908.
[19] E. Lindner, R. Gyurcsányi, Journal of Solid State Electrochemistry, 13 (2009) 51-68.
[20] S. Katsuta, K.-i. Nakamura, Y. Kudo, Y. Takeda, The Journal of Physical Chemistry B, 116 (2012) 852-859.
[21] M.G. Freire, C.M.S.S. Neves, P.J. Carvalho, R.L. Gardas, A.M. Fernandes, I.M. Marrucho, L.M.N.B.F. Santos, J.A.P. Coutinho, The Journal of Physical Chemistry B, 111 (2007) 13082-13089.
[22] A. Marciniak, Int. J. Mol. Sci., 11 (2010) 1973-1990.
[23] J. Ranke, A. Othman, P. Fan, A. Müller, Int. J. Mol. Sci., 10 (2009) 1271-1289.
[24] R. Gourishetty, A. Crabtree, W. Sanderson, R.D. Johnson, Anal Bioanal Chem, 400 (2011) 3025-3033.
[25] N. Abramova, A. Bratov, Sensors, 9 (2009) 7097-7110.
[26] J. Bobacka, A. Lewenstam, A. Ivaska, Journal of Electroanalytical Chemistry, 489 (2000) 17-27.
[27] A. Michalska, K. Maksymiuk, Journal of Electroanalytical Chemistry, 576 (2005) 339-352.
[28] B. Paczosa-Bator, J. Peltonen, J. Bobacka, A. Lewenstam, Analytica Chimica Acta, 555 (2006) 118-127.
[29] T.F. Otero, J. Arias-Pardilla, Electrochemical Devices: Artificial Muscles, in: S. Cosnier, A. Karyakin (Eds.) Electropolymerization, Wiley, 2011, pp. 241-245.

[30] G.G. Wallace, G.M. Spinks, L.A.P. Kane-Maguire, Assembly of Polypyrroles, in: Conductive Electroactive Polymers: Intelligent Polymer Systems, CRC Press, 2009, pp. 59-101.
[31] Merck, Ionic Liquids Brochure. Product Information, in, 2012, pp. 5.
[32] Y. Pan, L.E. Boyd, J.F. Kruplak, W.E. Cleland, J.S. Wilkes, C.L. Hussey, Journal of The Electrochemical Society, 158 (2011) F1-F9.
[33] J. Koryta, J. Dvořák, L. Kavan, Transport Processes in Electrolyte Systems, in: Principles of electrochemistry, Wiley, 1993, pp. 122.
[34] S. Ahmad, M. Deepa, S. Singh, Langmuir, 23 (2007) 11430-11433.
[35] S. Ahmad, T. Carstens, R. Berger, H.-J. Butt, F. Endres, Nanoscale, 3 (2011) 251-257.